



Contents lists available at ScienceDirect

Powder Technology

journal homepage: www.elsevier.com/locate/powtec

Preparation, characterisation of thermally treated Algerian dolomite powders and application to azo-dye adsorption

Fatima Boucif^a, Kheira Marouf-Khelifa^b, Isabelle Batonneau-Gener^c, Jacques Schott^d, Amine Khelifa^{a,*}^a Laboratoire de Structure, Elaboration et Applications des Matériaux Moléculaires, (S.E.A.2M.), Département de Chimie, Université de Mostaganem, B.P. 981, R.P., Mostaganem 27000, Algeria^b Laboratoire S.T.E.V.A., Département de Chimie, Université de Mostaganem, Algeria^c Laboratoire LACCO – UMR 6503, 40 avenue du Recteur Pineau, 86022 Poitiers, France^d Géochimie: Transferts et Mécanismes, Laboratoire LMTG (UMR 5563)-OMP-, Université Paul-Sabatier, Toulouse, France

ARTICLE INFO

Article history:

Received 4 September 2009

Received in revised form 31 March 2010

Accepted 9 April 2010

Available online xxxx

Keywords:

Dolomite

Thermal treatment

X-ray powder diffraction

SEM

Adsorption

ABSTRACT

Dolomite powder from Ouled Mimoun, Tlemcen (western region of Algeria) was thermally treated within the temperature range 450–1000 °C. The modifications undergone by dolomite, inherent to thermal treatment, were investigated from X-ray diffraction patterns. The results were also discussed using scanning electronic microscopy and nitrogen adsorption. The XRD data, analysed from X Pert Plus program, showed that the dolomite phase ceases at 700 °C and is relayed by the formation of in situ calcite and periclase. The crystallographic parameters of these two phases tend towards that of pure periclase and calcite at 1000 and 900 °C, respectively. SEM analysis indicated that the morphological properties were profoundly affected. SEM images of D-1000 (sample treated at 1000 °C) indicated that the original particle shape of dolomite (presence of discrete grains having sharp edges with presence of cleavages) was totally destroyed, leading to small spherical particles with a diameter of 0.1 µm. The specific surface area value of D-1000 increased more than 6 times against that of the raw dolomite. Adsorption of azo-dye Orange I from aqueous solutions onto untreated and treated dolomites was also reported. The isotherms were of L-type. The interaction was explained by electrostatic considerations between sulfonate groups of the dye (D-SO₃Na), which are dissociated in the aqueous system, and positively charged adsorption sites. The affinity of orange I for the dolomitic solids follows the sequence D-900 > D-1000 > D-800 > D-600 > raw dolomite. The maximum retention capacity shown by D-900 was explained and correlated with its crystallographic properties.

© 2010 Elsevier B.V. All rights reserved.

1. Introduction

Dolomite is an inexpensive material. Its structure contains alternating planes of Ca²⁺ and Mg²⁺ cations with ideal formula CaMg(CO₃)₂. Occasionally one element may have a slightly greater presence than the other [1]. Dolomite is an important industrial mineral. It is used as a source of both magnesium metal and magnesia in different branches of industry such as the food and pharmaceutical industries and the production of fertilizers, glass, and building materials. One of the main applications is in the field of refractory materials, in order to produce fire-resistant products, used in metallurgy, chemical and ceramic industries [2–4]. Dolomite was also used as transesterification catalyst for palm kernel oil [5] and adsorbents for substances such as iodine [6], dyes [7], copper(II) [8], lead(II) and cadmium(II) [9], CO₂ [10] and so on.

The majority of these applications implies the decomposition of dolomite, from where the necessity and interest of studying its stability as a function of temperature. This thermal processing is

accompanied by structural changes within the solid product [11], causing a significant change of the crystallographic, morphological and textural properties. Obviously, the modification in the interfacial properties of dolomitic solids improves their adsorption properties.

The objectives of this study were to investigate the modifications undergone by Algerian dolomite owing to thermal treatment and apply the decomposition products for removing azo-dye orange I from aqueous solutions. The dolomite was treated over the range 450–1000 °C. The thermally modified samples are called dolomitic solids. The powder XRD data were measured by fitting with pseudo-Voigt function through the X Pert Plus program. The results were also discussed using scanning electronic microscopy and nitrogen adsorption. Despite evidence in the literature of increased interest in low-cost adsorbents, no adsorption study of azo-dye on dolomitic solids has yet been published, in which the treatment temperature is considered as a pertinent parameter.

2. Experimental

The dolomite used in this study was supplied from the Ouled Mimoun deposit in Tlemcen (western Algeria). The composition of

* Corresponding author.

E-mail address: aminekhelifadz@yahoo.fr (A. Khelifa).

Table 1
Chemical composition of raw dolomite.

Oxide	CaO	MgO	Fe ₂ O ₃	SiO ₂	Al ₂ O ₃	MnO ₂	Cr ₂ O ₃
Percentage (%)	31.18	21.05	0.02	0.01	0.002	0.0015	0.01

this dolomite is very close to the formula $\text{CaMg}(\text{CO}_3)_2$. Its typical chemical composition in mass% determined by a Cameca SX-50 electronic microprobe is given in Table 1. The grain size of the material used was 0.125–0.25 mm. Samples of raw dolomite were heated in a muffle furnace from 450 to 1000 °C at a constant heating rate of 10 °C/min. Each sample was processed at the relevant temperature for 2 h [12]. Mineralogical species of raw dolomite and dolomitic solids were characterised by X-ray powder diffraction employing an INEL CPS 120 diffractometer using monochromated $\text{CuK}\alpha$ radiation. The XRD data were collected over a 2θ range of 10–70° with a step width of 0.02°. Peak intensities and angle positions were measured by fitting with pseudo-Voigt function through the X Pert Plus program. This program also has a facility for profile fitting and decomposition of overlapping diffractions. The molar concentration of CaCO_3 , X_{Ca} , in dolomite was calculated using its linear dependence on lattice parameters. The formula [13]:

$$X_{\text{Ca}} = \frac{(d_{104} - 2.8840)}{0.003} + 50 \quad (1)$$

expresses the linear dependence of d_{104} of dolomite with respect to the fix-point of ideal stoichiometric dolomite. The d_{104} value of the Ouled Mimoun dolomite is 2.8847 Å, corresponding to $X_{\text{Ca}} = 50.23\%$. This again confirms that the dolomite has a stoichiometry close to $(\text{Ca}/\text{Mg}) = 1$, with a formula $\text{CaMg}(\text{CO}_3)_2$.

The crystallite size and morphology of the samples were determined by scanning electronic microscopy (JEOL, JSM-6360, Japan). The nitrogen adsorption isotherms were measured at 77 K via an ASAP 2010 instrument (Micromeritics, Norcross, GA, USA) using helium and nitrogen of 99.99% purity. The specific surface areas were calculated using the standard BET method.

The adsorption experiments were performed via the batch method at 25 ± 1 °C. 0.06 g of dolomitic adsorbents was mixed with 20 mL of aqueous orange I solution in a concentration range of 20–200 mg/L. pH of the dispersions was adjusted to 5 by adding 0.1 M HCl. After equilibration, the solution was separated by filtration. Volumes of 10 mL aliquot of the supernatant were analysed by visible spectrophotometry at 476 nm using a Hach DR 2800 visible spectrophotometer. The adsorbed amount was determined from the difference between the initial and final concentrations. Preliminary studies were carried out to optimise the time of equilibrium, pH and the adsorbent concentration. Orange I ($\text{C}_{16}\text{H}_{11}\text{N}_2\text{OSO}_3\text{Na}$, $\text{pK}_a = 8.2$, analytical grade) was purchased from Fluka.

3. Results and discussion

The data of the untreated dolomite collected at room-temperature led to the cell parameters $a = b = 4.8076$ Å, $c = 16.0103$ Å, $\alpha = \beta = 90^\circ$, $\gamma = 120^\circ$ and $V = 320.47$ Å³, for a rhombohedral cell in the $R\bar{3}$ space group. Examination of the untreated Eugui dolomite by XRD also

Table 2
Crystallographic parameters of various dolomites.

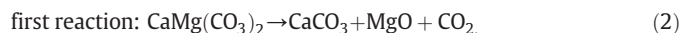
a (Å)	c (Å)	V (Å ³)	References
4.8076	16.010	320.47	This study
4.8072	16.005	320.31	[15]
4.8089	16.015	320.75	[16]
4.8033	15.984	319.30	[17]
4.8069	16.002	320.20	[18]

Table 3
Crystallographic parameters of the thermally treated dolomite samples.

Temperature (°C)	a (Å)	c (Å)	V (Å ³)
450	4.8123	16.112	323.13
500	4.8138	16.142	323.93
550	4.8159	16.158	324.53
600	4.8180	16.169	325.04
650	4.8222	16.204	326.31
700	4.8271	16.231	327.52

showed that the material crystallises in the $R\bar{3}$ space group [14]. The parameters relating to the dolomite from Ouled Mimoun agree closely with those reported in the scientific literature for other stoichiometric dolomites. The comparison is given in Table 2.

These unit-cell parameters for the thermally treated dolomites are reported in Table 3 and depicted in Figs. 1 and 2. The a and c cell parameters uniformly increase with temperature up to 700 °C, although not linearly. Similar evolution was observed by Reeder and Markgraf [18] for dolomite from Eugui (Spain). Above 700 °C, a saw-tooth evolution was obtained (data not shown), revealing a structural discontinuity that would indicate a phase transition. The latter is the consequence of beginning of the dolomite decarbonation. The decomposition of dolomite has been extensively studied, mainly by TGA or DTA, because of its mineralogical interest and industrial importance. According to the literature data [19], the thermal decomposition of dolomite occurs in air in two steps, as follows:



The decomposition of dolomite above 700 °C, corresponding to the first reaction, leads to changes in the chemical composition of the surface and in the porosity of this mineral [20]. The second reaction proceeds from 900 °C. Generally, the product of partial decomposition of dolomite (reaction (2)) consists of a rigid porous calcite and the fine powdered magnesium oxide [21]. Consequently, we followed from 700 °C the crystallographic parameters of calcite and magnesium oxide (Table 4).

Fig. 3 shows that the a cell parameter, for in situ formed calcite, increases from 750 to 800 °C. This evolution could be explained by the formation of an intermediate solid solution, $\text{Ca}_{(1-x)}\text{Mg}_x(\text{CO}_3)$. The increase in the cell parameters from 750 °C, would be explained by the release of Mg^{2+} from the solid solution. The existence of a

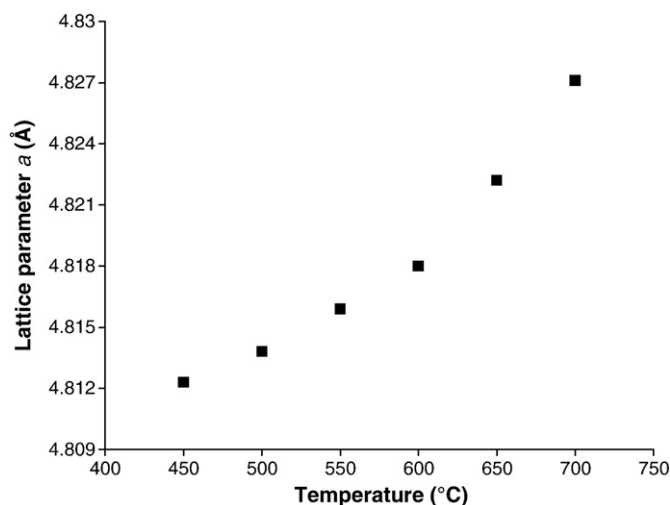


Fig. 1. Variation of a unit-cell parameter of dolomite versus temperature.

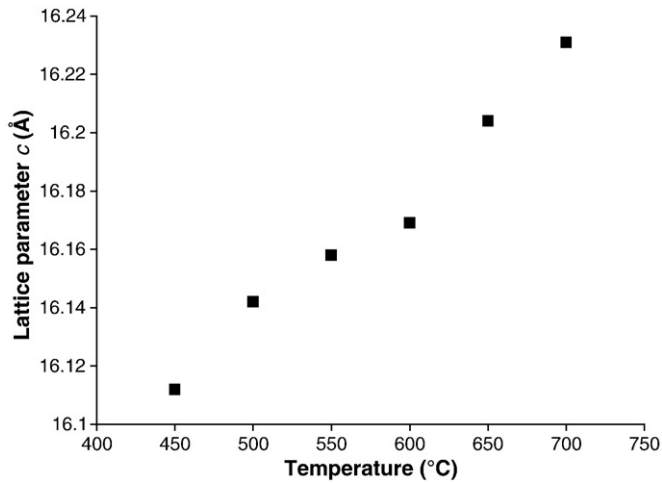


Fig. 2. Variation of *c* unit-cell parameter of dolomite versus temperature.

magnesium-rich calcite has been reported by Goldsmith and Heard [22]. These authors found a calcite phase with 20 mol% of magnesium at 900 °C. Galai et al. [23] studied the mechanism of growth of MgO and CaCO₃ during a dolomite partial decomposition. They found that at 680 °C and under 0.025 atm, the reaction product is a solid solution Ca_(1-x)Mg_x(CO₃). The final content was estimated to be *x* = 0.052. From 800 to 900 °C (Fig. 3), the reached value tends towards that of pure calcite phase. As temperature increases, the *x* variable tends towards zero, so that the solid solution approaches stoichiometry of a pure calcite. The increase of the calcite cell parameters with temperature, calcite crystallised over a host dolomite structure, was also reported by De Aza et al. [16]. From 900 °C, the found reflections do not correspond to that of calcite, probably because of its lime decomposition.

The *a* crystallographic parameter of in situ formed periclase phase, resulting from the thermal decomposition of dolomite, drastically decreases between 750 and 800 °C. The reached value tends towards that of pure periclase, from 800 to 1000 °C (Fig. 4). The strong reduction observed at the beginning is due to the fact that magnesium ions are released from a solid solution as discussed above. As temperature increases, the growth of the MgO phase induces a shrinkage of the *a* parameter from 4.305 to 4.217 Å (Table 4), the Mg²⁺ cation (*r*_{Mg}²⁺ = 0.65 Å) being smaller than Ca²⁺ (*r*_{Ca}²⁺ = 0.99 Å). The Mg–O bond length is therefore smaller than that the Ca–O bond.

In order to characterise the structural changes caused by thermal modification within the bulk and surface, SEM micrographs of the grain cross-sections were also reported. These are presented in Fig. 5 for the raw dolomite and for the samples treated at 800 (D-800) and 1000 °C (D-1000). The sample a (Fig. 5a) shows the presence of discrete grains with some grains having sharp edges. An identical morphology was also reported by Samtani et al. [24]. Fig. 5b indicates that the dolomite presents cleavages and shows an apparent preferential orientation of dolomite crystals, along *c*-axis. Dolomite

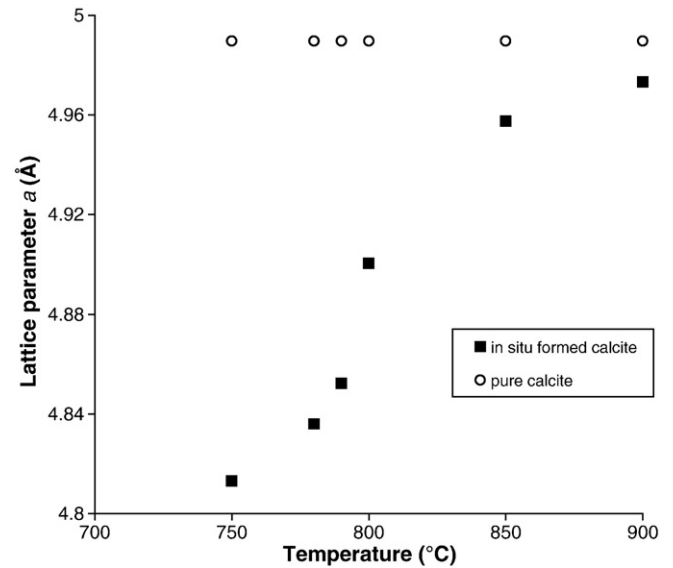


Fig. 3. Variation of *a* cell parameter versus temperature for in situ formed calcite.

belongs to the rhombohedral crystalline system which has a threefold inversion axis and therefore is anisotropic. It should be noted that the bright area in Fig. 5c is an inclusion of calcite and quartz. It was mentioned in a previous paper that the Ouled Mimoun dolomite contained traces of quartz [25]. After thermal modification, the morphological properties were profoundly affected, causing a significant change of the surface topography of the samples. Micrographs of sample D-800 (Fig. 5d and e) clearly show the newly created pores and slots. The structure appears to be less compact than that of the starting material. These features could be explained by the decarbonation of MgCO₃ associated with dolomite as shown in reaction (2). The CO₂ release led to a more porous structure. Scanning electron micrographs of D-1000 (Fig. 5f and g) showed that the original particle shape of dolomite is totally destroyed by the thermal treatment at 1000 °C, forming small spherical particles with a diameter of 0.1 μm. D-1000 thus has a porous structure which resembles a sponge. The fragmentation of the particles and the formation of spherical shape were also evidenced by SEM images for a mechanically activated dolomite [26].

Results relating to the specific surface area of the natural dolomite and the modified thermally dolomites are summarised in Table 5.

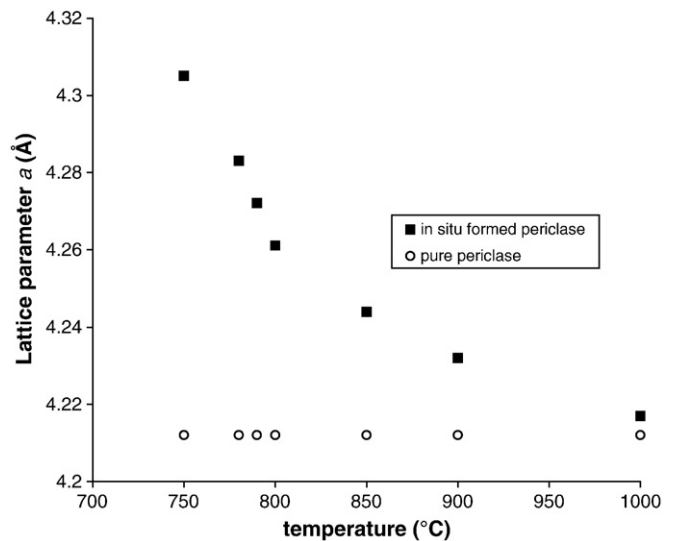


Fig. 4. Variation of *a* cell parameter versus temperature for in situ formed periclase.

Table 4
Variation of unit cell with temperature for in situ formed calcite and periclase.

Temperature (°C)	Unit cell for in situ formed calcite			Unit cell for in situ formed periclase	
	<i>a</i> (Å)	<i>c</i> (Å)	<i>V</i> (Å ³)	<i>a</i> (Å)	<i>V</i> (Å ³)
750	4.8131	16.956	340.17	4.305	79.78
780	4.8360	16.974	343.78	4.283	78.57
790	4.8522	17.145	349.57	4.272	77.96
800	4.9003	17.275	359.24	4.261	77.36
850	4.9574	17.311	368.42	4.244	76.44
900	4.9732	17.385	372.36	4.232	75.79
1000	–	–	–	4.217	74.99

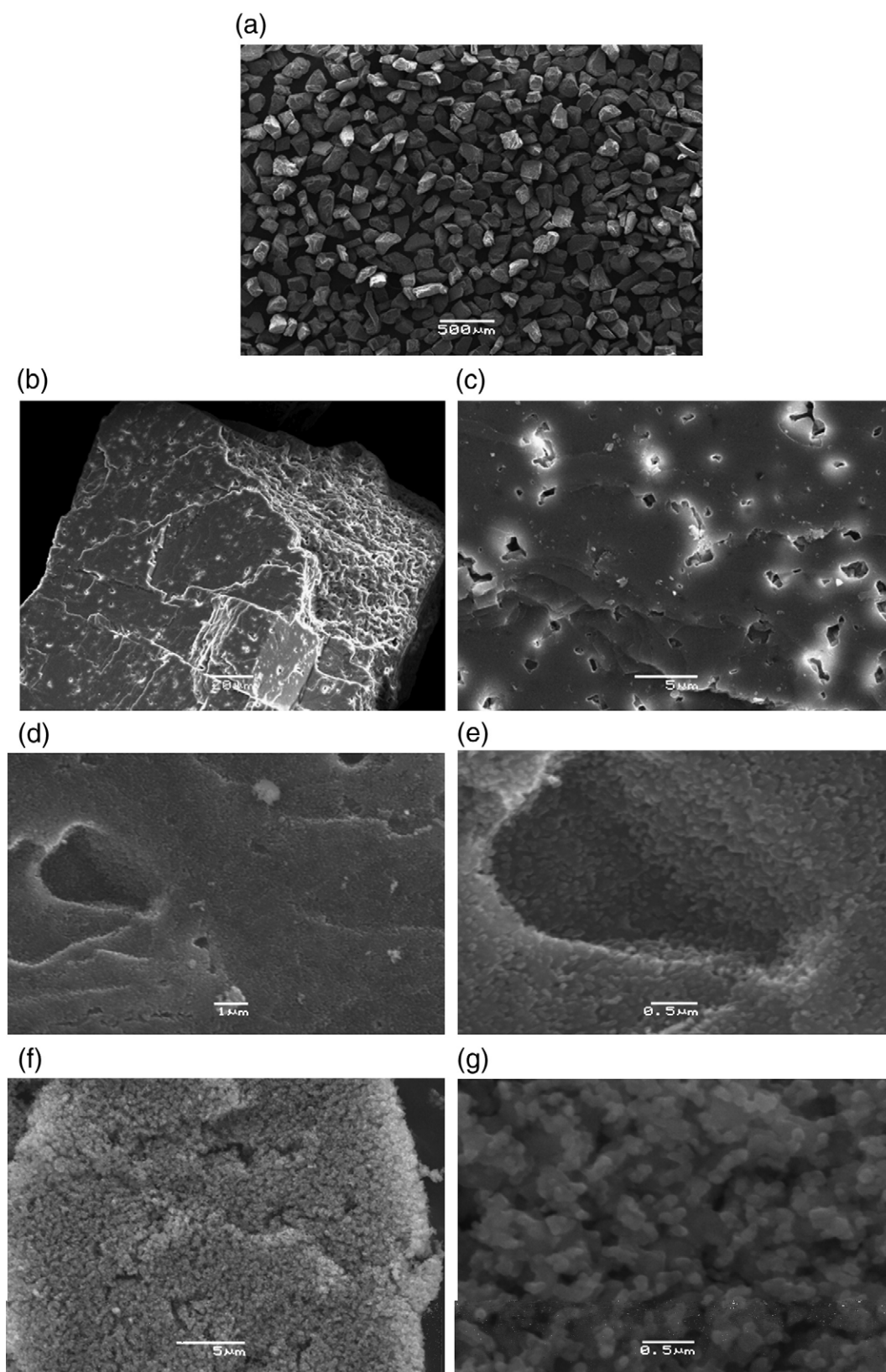


Fig. 5. SEM images of : (a: magnif. $\times 30$), (b: magnif. $\times 650$) and (c: magnif. $\times 3700$) untreated dolomite; (d: magnif. $\times 10,000$) and (e: magnif. $\times 27,000$) dolomite treated at 800 °C; (f: magnif. $\times 4000$) and (g: magnif. $\times 30,000$) dolomite treated at 1000 °C.

Specific surface area increases with treatment temperature reaching a maximum of 11.36 m²/g at 1000 °C. A value of 11 m²/g was also attained for a dolomite milled during 21 hr [27]. The lowest value was found for the untreated dolomite. The value of the D-1000 sample was

more than six times higher than that of the raw dolomite, for a particle size of 125–250 μm. Dolomite with a mean particle size of 100 μm produced a surface area of 19.5 m²/g, once treated at 800 °C [8]. A value of 7.1 m²/g was found at 850 °C, for a particle size distribution

Table 5

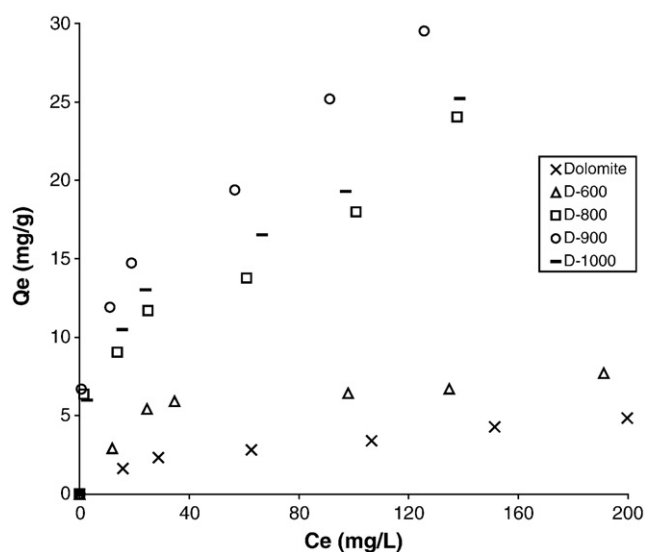
Specific surface area of the thermally treated dolomite samples.

Sample	Heating temperature (°C)	Specific surface area (m ² /g)
Raw dolomite	–	1.82
D-600	600	2.45
D-800	800	9.34
D-900	900	9.77
D-1000	1000	11.36

ranging between 1000 and 1200 μm [28]. This indicates that the particle size of the dolomite has a significant effect on the activation process. The mechanism proposed for the particles large size is that there exists an un-reacted core made up of dolomite surrounded by a surface layer constituted by the products of the reaction (1) or (2), according to the treatment temperature. From mechanistic studies, it was proved that the thermal dissociation of dolomite begins at the solid surface and extends over time until the interior of the particle is reached [29].

Thermal modification leads thus to a considerable change in the interfacial properties of dolomitic adsorbents. From these considerations, it is clear that a thermally dolomite treated has a greater potential to act as an adsorbent, in spite of a relatively low surface area, compared to commercial adsorbents.

For illustrating the improvement of the adsorptive properties of thermally modified dolomites, we reported the results of the orange I adsorption. The experiments have been repeated three times. For each experiment, the mean value was considered. The results were determined with a variation coefficient lower than 5%. Adsorption isotherms are depicted in Fig. 6 and were of L-type according to Giles et al. [30]. This isotherm shape indicates that there is no strong competition between the solvent and the adsorptive for surface sites. As more surface sites are occupied, it becomes increasingly difficult for the adsorptive to find a vacant site, at least for raw dolomite and D-600. The isotherms for the D-800, D-900 and D-1000 samples do not reach a limiting value. This could be explained by increasing of number of positively charged sites available inside these solids. In the aqueous system, sulfonate groups of the dye (D-SO₃Na) are dissociated and the dye becomes anionic. The surface charge of materials changes according to the condition of the aqueous dispersion and is usually explained in terms of a point of zero charge (pH_{zpc}). In a previous study [25], we found that isoelectric point of the Ouled Mimoun dolomite was approximately 6.8. At pH 5, high electrostatic attractions exists between negative charges of orange I and positively charged adsorption sites.

**Fig. 6.** Adsorption isotherms of orange I onto dolomitic solids at 25 °C.

Such interactions were also considered between pentachlorophenol and dolomitic adsorbents [31]. According to Chen and Tao [32], below pH 6.8 dolomite is positively charged due to prevalence of the species $[\text{MgOH}^+]$ and $[\text{CaOH}^+]$.

The affinity follows the sequence $\text{D-900} > \text{D-1000} > \text{D-800} > \text{D-600} > \text{raw dolomite}$. The uptake capacity of D-900 is 6 times higher than that of the untreated dolomite. As shown from Fig. 3, the a cell parameter for in situ formed calcite tends towards that of pure calcite phase. This means that the dolomitic adsorbent, treated at 900 °C, consists of pure calcite phase and magnesium oxide. Nyström et al. [33] showed that no isoelectric point (IEP) was observed for calcite in water and that ζ -potential at a pH slightly below 8 was around 25 mV. Electrophoretic measurements of synthetic calcite dispersions revealed that the positive ζ -potential, at $\text{pH} < 9.5$, was the result of the prevailing positive ionic species (Ca^{2+} , CaHCO_3^+ , CaOH^+) at the calcite–aqueous solution interface [34]. Cicerone et al. [35] showed that in the case of $\text{Mg}^{2+}/\text{CaCO}_3$ system, magnesium ions alter the surface charge of CaCO_3 by incorporation into the calcite lattice, yielding a more positively charged surface. From these considerations, the highest capacity of orange I retention by D-900 could be explained by the great number of charged positively active sites, due to in situ formed calcite, associated to those generated at magnesium oxide–aqueous solution interface.

4. Conclusion

X-ray diffraction patterns for the thermally treated dolomite samples were investigated over the range 450–1000 °C. The data of the untreated dolomite collected at room-temperature led to the cell parameters $a = b = 4.8076 \text{ \AA}$, $c = 16.0103 \text{ \AA}$, $\alpha = \beta = 90^\circ$, $\gamma = 120^\circ$ and $V = 320.47 \text{ \AA}^3$, for a rhombohedral cell in the $R\bar{3}$ space group. The follow-up of cell parameters of the thermally treated samples, identified as dolomitic solids, showed that the dolomite phase ceases at 700 °C and is relayed by the formation of in situ calcite and periclase. The crystallographic parameters of these two phases tend towards that of pure periclase and calcite at 1000 and 900 °C, respectively. From 900 °C, the found reflections do not correspond to that of calcite, probably because of its lime decomposition.

SEM analysis for the untreated dolomite revealed the presence of discrete grains having sharp edges with presence of cleavages and a preferential orientation along c -axis. Micrographs of the sample D-800 clearly showed the newly created pores and slots. SEM images of D-1000 indicated that the original particle shape of dolomite was totally destroyed by the thermal treatment at 1000 °C, forming small spherical particles with a diameter of 0.1 μm . Specific surface area increased with treatment temperature reaching a maximum of 11.36 m²/g at 1000 °C. The thermally modified dolomites showed a high affinity for orange I adsorption. The process was explained by electrostatic considerations between the negatively charged orange I dye and the positively charged adsorption sites. The uptake capacity of D-900 was 6 times higher than that of the untreated dolomite, namely 29.5 against 4.8 mg/L. These results indicate that dolomitic solids are potentially cost effective materials for azo-dyes adsorption.

References

- [1] R.S. Boynton, Chemistry and Technology of Lime and Limestone, Interscience Publishers, New York, 1967.
- [2] H.A. Yeprem, E. Türedi, S. Karagöz, A quantitative-metallographic study of the sintering behaviour of dolomite, Mater. Charact. 52 (2004) 331–340.
- [3] G.S. Gai, Y.F. Yang, S.M. Fan, Z.F. Cai, Preparation and properties of composite mineral powders, Powder Technol. 153 (2005) 153–158.
- [4] M. Rabah, E.M.M. Ewais, Multi-impregnating pitch-bonded Egyptian dolomite refractory brick for application in ladle furnaces, Ceram. Int. 35 (2009) 813–819.
- [5] C. Ngamcharussrivichai, W. Wiwatnimit, S. Wangnoi, Modified dolomites as catalysts for palm kernel oil transesterification, J. Mol. Catal. A: Chem. 276 (2007) 24–33.

- [6] S.F. Estefan, M.B. Morsi, G.A. El-Shobaky, I.F. Hewaidy, The role of calcination temperature in iodine adsorption by different magnesium oxide powders, *Powder Technol.* 49 (1987) 143–147.
- [7] G.M. Walker, L. Hansen, J.A. Hanna, S.J. Allen, Kinetics of a reactive dye adsorption onto dolomitic sorbents, *Water Res.* 37 (2003) 2081–2089.
- [8] G.M. Walker, G. Connor, S.J. Allen, Copper II removal onto activated dolomite, *Chem. Eng. Res. Des.* 82 (2004) 961–966.
- [9] S. Kocaoba, Comparison of amberlite IR 120 and dolomite's performances for removal of heavy metals, *J. Hazard Mater* 147 (2007) 488–496.
- [10] S. Stendardo, P.U. Foscolo, Carbon dioxide capture with dolomite: a model for gas-solid reaction within the grains of a particulate sorbent, *Chem. Eng. Sci.* 64 (2009) 2343–2350.
- [11] B. Bilinski, E. Stefaniak, P. Staszczuk, The influence of thermal activation on the surface properties of dolomite, *Powder Technol.* 73 (1992) 261–266.
- [12] E. Stefaniak, B. Bilinski, P. Staszczuk, Physicochemical study of dolomitic sorbents prepared under different thermal conditions. Part I. The influence of temperature, *Adsorpt Sci. Technol* 17 (1999) 85–95.
- [13] A. Kleesment, A. Shogenova, Lithology and evolution of Devonian carbonate and carbonate-cemented rocks in Estonia, *Proc. Estonian Acad. Sci. Geol.* 54 (2005) 153–180.
- [14] R.J. Reeder, H.R. Wenk, Structure refinements of some thermally disordered dolomites, *Am. Mineral.* 68 (1983) 769–776.
- [15] S.M. Antao, W.H. Mulder, I. Hassan, W.A. Crichton, J.B. Parise, Cation disorder in dolomite, $\text{CaMg}(\text{CO}_3)_2$, and its influence on the aragonite + magnesite \leftrightarrow dolomite reaction boundary, *Am. Mineral.* 89 (2004) 1142–1147.
- [16] A.H. De Aza, M.A. Rodriguez, J.L. Rodriguez, S. De Aza, P. Pena, P. Convert, T. Hansen, X. Turrillas, Decomposition of dolomite monitored by neutron thermodiffraction, *J. Am. Ceram. Soc.* 85 (2002) 881–888.
- [17] P.L. Althoff, Structural refinements of dolomite and a magnesian calcite and implications for dolomite formation in the marine environment, *Am. Mineral.* 62 (1977) 772–783.
- [18] R.J. Reeder, S.A. Markgraf, High-temperature crystal chemistry of Dolomite, *Am. Mineral.* 71 (1986) 795–804.
- [19] H.G. Wiedemann, G. Bayer, Note on the thermal decomposition of dolomite, *Thermochim Acta* 121 (1987) 479–485.
- [20] P. Staszczuk, E. Stefaniak, B. Bilinski, E. Szymanski, R. Dobrowolski, S.A.A. Jayaweera, Investigations on the adsorption properties and porosity of natural and thermally treated dolomite samples, *Powder Technol.* 92 (1997) 253–257.
- [21] S. Karaca, A. Gürses, M. Ejder, M. Açıkyıldız, Adsorptive removal of phosphate from aqueous solutions using raw and calcinated dolomite, *J. Hazard. Mater.* 128 (2006) 273–279.
- [22] J.R. Goldsmith, H.C. Heard, Subsolidus phase relations in the system $\text{CaCO}_3\text{--MgCO}_3$, *J. Geol.* 69 (1961) 45–74.
- [23] H. Galai, M. Pijolat, K. Nahdi, M. Trabelsi-Ayadi, Mechanism of growth of MgO and CaCO_3 during a dolomite partial decomposition, *Solid State Ionics* 178 (2007) 1039–1047.
- [24] M. Samtani, E. Skrzypczak-Jankun, D. Dollimore, K. Alexander, Thermal analysis of ground dolomite, confirmation of results using an X-ray powder diffraction methodology, *Thermochim Acta* 367 (2001) 297–309.
- [25] R. Marouf, K. Marouf-Khelifa, J. Schott, A. Khelifa, Zeta potential study of thermally treated dolomite samples in electrolyte solutions, *Micropor Mesopor Mater* 122 (2009) 99–104.
- [26] É. Makó, The effect of quartz content on the mechanical activation of dolomite, *J. Eur. Ceram. Soc.* 27 (2007) 535–540.
- [27] R.B. Gammage, D.R. Glasson, I.R. Hodgson, P. O'Neill, Microcrystalline structure of milled dolomite and its constituent carbonates, *J. Colloid Interface Sci.* 92 (1983) 530–544.
- [28] A. Duffy, G.M. Walker, S.J. Allen, Investigations on the adsorption of acidic gases using activated dolomite, *Chem. Eng. J.* 117 (2006) 239–244.
- [29] M. Hartman, O. Trnka, V. Vesely, K. Svoboda, Predicting the rate of thermal decomposition of dolomite, *Chem. Eng. Sci.* 51 (1996) 5229–5232.
- [30] C.H. Giles, T.H. Mac Ewan, S.N. Makhwa, D. Smith, Studies in adsorption. Part XI. A system of classification of solution adsorption isotherms and its use in diagnosis of adsorption mechanisms and in measurement of specific surface areas of solids, *J. Colloid Interface Sci.* 3 (1960) 3973–3993.
- [31] R. Marouf, N. Khelifa, K. Marouf-Khelifa, J. Schott, A. Khelifa, Removal of pentachlorophenol from aqueous solutions by dolomitic sorbents, *J. Colloid Interface Sci.* 297 (2006) 45–53.
- [32] G. Chen, D. Tao, Effect of solution chemistry on flotability of magnesite and dolomite Int, *J. Miner. Process.* 74 (2004) 343–357.
- [33] R. Nyström, M. Lindén, J.B. Rosenholm, *J. Colloid Interface Sci.* 242 (2001) 259–263.
- [34] N. Vdović, J. Biščan, Electrokinetics of natural and synthetic calcite suspensions, *Colloid Surf. A.* 137 (1998) 7–14.
- [35] D.S. Cicerone, A.E. Regazzoni, M.A. Blesa, Electrokinetic properties of the calcite/water interface in the presence of magnesium and organic matter, *J. Colloid Interface Sci.* 154 (1992) 423–433.